PCCP

Cite this: *Phys. Chem. Chem. Phys.*, 2011, **13**, 14176–14182

www.rsc.org/pccp

PAPER

Dimers of cyclic carbonates: chirality recognition in battery solvents and energy storage†

Franz Kollipost, Susanne Hesse, Juhyon J. Lee and Martin A. Suhm*

Received 6th May 2011, Accepted 12th May 2011
DOI: 10.1039/c1cp21460h

Dimers of ethylene carbonate and propylene carbonate are created in supersonic jet expansions and characterized by FTIR spectroscopy. Fermi resonances are switched on and off by dimerization. There is a unique centrosymmetric dimer of ethylene carbonate in a pronounced case of complementary chirality synchronization, contributing to its energy storage capacity at melting. Two chiral propylene carbonate molecules combine in more intricate ways. If they have the same handedness, one of them is forced into an axial conformation and the binding partner stays in the more stable equatorial structure. If they have opposite handedness, centrosymmetric dimers of either axial or equatorial conformations are formed. This suggests the usefulness of chirality control in elucidating ionic transport mechanisms in battery solvents and asymmetric catalysis in such solvents.

1 Introduction

Organic carbonates are highly polar, if the two alkyl groups are joined into a small ring and thus forced into a *trans* position relative to the carbonyl group. This is the key for their excellent solvent properties, including a wide liquid range and a dielectric constant comparable to that of water. The simplest representative ethylene carbonate (EC, see Fig. 1) has a melting point slightly above room temperature. Combined with suitable additives, it is a potential temperature management material for buildings, due to its large heat of fusion and liquid range, which at the same time could help in the carbon capture project.[1] The chiral derivative propylene carbonate (PC) melts far below 0 °C but shares with EC a normal boiling point close to 250 °C. It is a popular, low-toxicity and low-flammability solvent for Li batteries. Furthermore, it is used in catalysis, natural gas processing and cosmetics.[2,3] The most elementary supramolecular building blocks of these green solvents, molecular dimers, have not been structurally studied in the gas phase, so far. This may be related to their potential to form non-polar antiparallel dipole–dipole stacks, which make them difficult to study by microwave spectroscopy.[4]

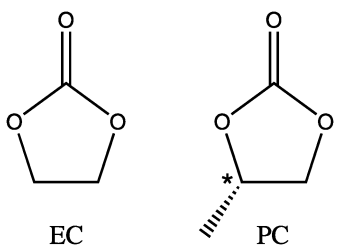

Fig. 1 Structures of EC and (*S*)-PC.

Here, we present the first infrared study of EC and PC dimers in supersonic jet expansions, together with the corresponding cold monomer spectra. We offer straightforward structural explanations of the spectral signatures, including chirality recognition aspects in the flexible PC case. The interaction between the monomers is dominated by electrostatic forces. Therefore, quantum chemistry based on hybrid functionals and MP2 perturbation theory is expected to provide a reliable description of the way in which two molecules interact, whereas a HF treatment was shown to be somewhat inferior.[5] While we see our experimental work as an ultimate reference for the testing of highly accurate electron correlation treatments, we thus use B3LYP and MP2 calculations with the 6-311++G(d,p) basis set as structural assignment tools in the present study. In addition we have explored the empirically dispersion-corrected B97-D functional.[6] Experimentally, it would be most desirable to combine Raman and IR spectroscopy. As the low volatility of EC and PC still presents a challenge for Raman gas phase dimer studies,[7,8] we focus on FTIR spectra in this investigation.

2 Methods

Our technique involves the expansion of a low concentration mixture of the carbonate (EC, ABCR, 99%; (*S*)-PC, ABCR, 98%; racemic PC, Acros Organics, 99.5%) in He (Linde, 99.996%)

Institut für Physikalische Chemie, Universität Göttingen, Tammannstr. 6, 37077 Göttingen, Germany.
E-mail: msuhm@gwdg.de; Fax: +49 551 393117
† Electronic supplementary information (ESI) available: Spectroscopic data, candidates for the EC Fermi resonance and discussion of the fingerprint range of PC. See DOI: 10.1039/c1cp21460h

through a pulsed slit nozzle into a large vacuum chamber, where supersonic cooling down to temperatures of a few tens of K creates tightly bound dimers and removes spectral contributions from thermally excited molecules. The sub-second gas pulses are synchronized to interferometer scans of a Bruker IFS 66v/S FTIR instrument and separated by a waiting time on the order of tens of seconds, during which the vacuum conditions are recovered by a series of mechanical pumps. If the He is saturated with the carbonate below room temperature (at a vapor pressure of less than 0.03 mbar[9]), the expansion is dominated by cold monomers and a 60 cm slit nozzle is employed for maximum sensitivity. If saturation takes place at elevated temperatures,[10] the expansion also contains dimers and smaller amounts of trimers, which can usually be discriminated from the dimers by their faster concentration growth law. In this case, a twin nozzle of only 1 cm length is sufficient and easier to heat homogeneously.

The calculations have been carried out using the Gaussian 03 (B3LYP, MP2) and 09 (B97D) program suites.[11]

3 Results

3.1 Ethylene carbonate (EC)

Fig. 2 shows EC spectra recorded in the room temperature gas phase, in the cold monomer-dominated expansion and in the heated expansion, concentrating on the spectral ranges where the C═O stretch (C) and the antisymmetric O–C–O (B) stretch as well as the symmetric CH_2–O (A) stretch are expected. Indeed, three rather strong bands are detected and their rotational profile and position unambiguously identifies them in the listed sequence, from higher to lower wavenumber. There is no evidence for pronounced Fermi resonance, which can be so frequent in the related lactones.[12] In the monomer-dominated jet expansion, the almost complete collapse of rotational structure allows for a rotational temperature estimate of 10–15 K. In the heated expansions (nozzle temperature 70/80/100 °C, compound temperature 50/60/80 °C), the rotational temperature (estimated from the contours) has increased to 25–35 K due to the heat of clustering and the increased starting temperature. These estimates are based on the approximate $\sqrt{T}$ dependence of the P/R-branch separation and the room temperature calibration. The cluster features in trace c appear with bathochromic (red) shift in the C═O range, with hypsochromic (blue) shift in the antisymmetric O–C–O stretching mode and with slight red shift for the symmetric CH_2–O stretching mode. Assuming similar intramolecular band strength in the clusters, close to 50% of the molecules are clustered under the strongest clustering conditions. As C═O band strengths tend to increase with

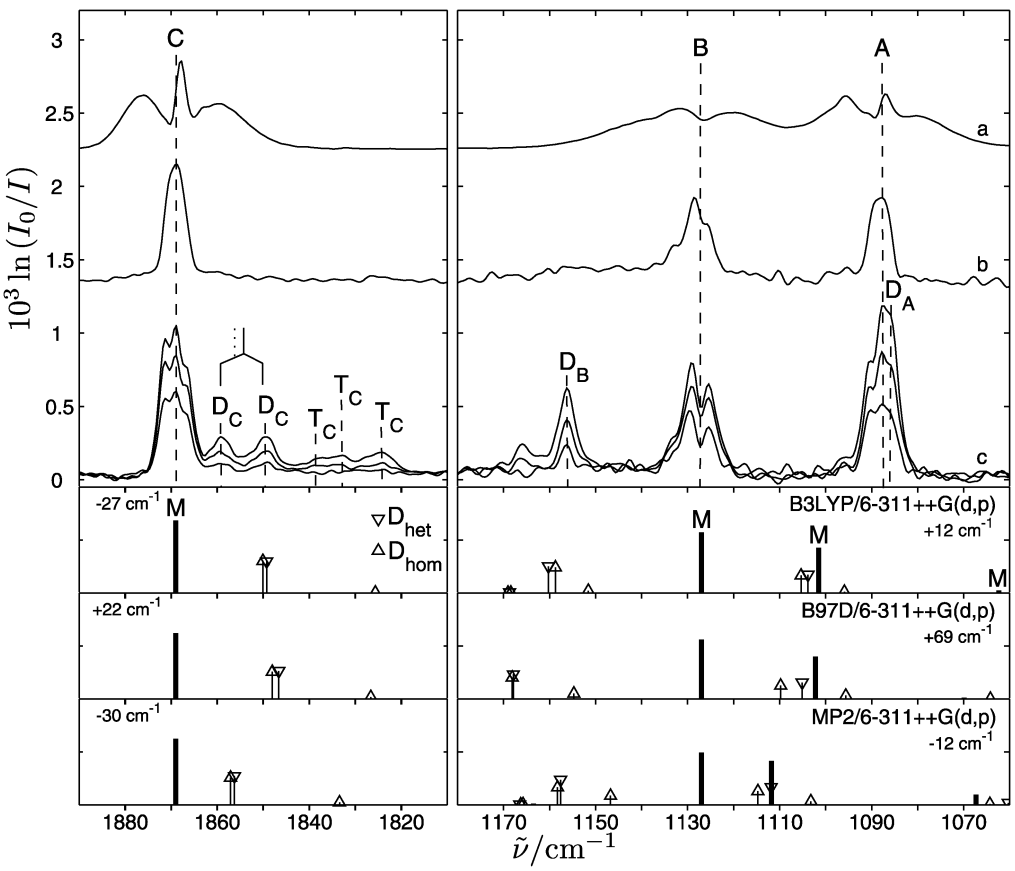

Fig. 2 Experimental spectra of EC in the carbonyl (C) and C–O range (×2) (A, B) together with harmonic predictions: (a) gas phase (×0.05); (b) monomer-dominated jet spectrum, 600 mm nozzle, ~1 bar stagnation pressure; (c) heated jet spectra at increasing temperature and thus concentration, revealing dimer (D) and trimer bands (T). The simulations in the bottom traces assume 17% D_{het}, 17% D_{hom} and 67% M. Calculated wavenumbers were uniformly shifted in the spectral windows, so that monomer bands (M) coincide for C and B, respectively. The values of the shifts are given in the windows of the calculated frequencies. See also Table S1 in the ESI.†

clustering, this may be a slight overestimate. Nevertheless, one expects significant amounts of trimers under these conditions. In the C=O stretching range, it is clear that the most red-shifted bands marked T are due to such trimers or larger aggregates. Such an assignment is also likely for the most blue-shifted band in the antisymmetric stretching region, whereas the spectral overlap in the symmetric stretch allows for no conclusion.

This supports a single dimer conformation or else a perfect spectral overlap among several dimer conformations. As EC monomer occurs in two enantiomeric puckered C_2-symmetric conformations which are separated by a barrier of less than 3 kJ mol^{-1},[4] several possible dimer structures may be conceived. This kind of isomerism has previously been overlooked.[13,14] In particular, only a homochiral pairing has been considered in an earlier study.[13] However, an exploration of the potential energy hypersurface at the MP2 and B3LYP levels reveals a single dimer conformation D_{het} within an energy window of 5 kJ mol^{-1} (MP2 energies, see Table 1). It consists of two monomers of opposite handedness which arrange themselves in a slipped head-to-tail structure with inversion symmetry. In this structure (shown in Fig. 3), the two C–O–C=O sequences are aligned, much like in the related case of γ-butyrolactone.[12] The next-lowest homochiral structure D_{hom} which we found involves a less perfect overlap and is predicted 6.1 kJ mol^{-1} (MP2), 4.5 kJ mol^{-1} (B97D) and 1.3 kJ mol^{-1} (B3LYP) higher in energy. It is conceivable that this structure relaxes to the heterochiral global minimum *via* the low barrier pathway discussed above. The driving force for this chirality synchronization process[15] is remarkably large. The inversion-symmetric dimer sandwich motif is also found in the crystal,[16] where neighboring dimers arrange in infinite antiparallel planes with uniform dipole orientation.

Table 1 Dimer dissociation energies without (D_e) and with (D_0) zero point correction in kJ mol^{-1} relative to the most stable monomers using the 6-311++G(d,p) basis set

	B3LYP		B97D		MP2	
Dimer	D_e	D_0	D_e	D_0	D_e	D_0
EC D_{het}	30.2	26.5	47.6	42.5	56.4	52.0
EC D_{hom}	28.7	25.2	43.0	38.0	50.0	45.9
PC D_{het}^{ee}	29.5	26.2	48.0	43.6	58.1	53.9
PC D_{het}^{aa}	27.0	24.0	46.8	42.0	56.5	52.5
PC D_{het2}^{aa}	26.1	22.9	46.5	41.4	55.6	51.4
PC D_{hom}^{ae}	27.8	24.9	47.6	42.5	57.4	53.3
PC D_{hom2}^{ae}	27.8	24.7	47.0	41.8	56.5	52.2

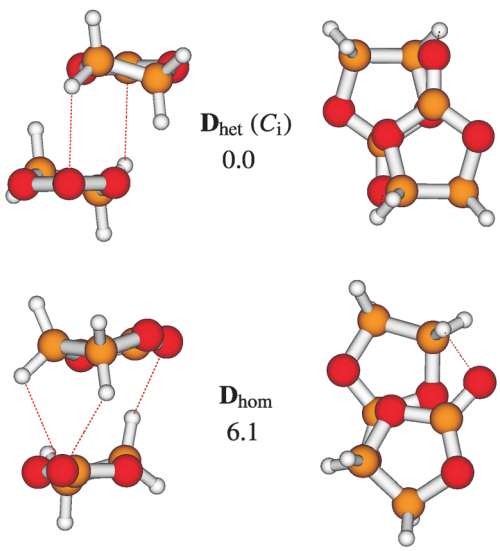

Fig. 3 Dimers of EC with relative MP2/6-311++G(d,p) energies ΔE_0 in kJ mol^{-1}, including zero-point correction.

The spectral predictions are also presented in Fig. 2 after shifting the harmonic values such that the monomer coincides with the experimentally observed monomer bands C and B. Note that the harmonic monomer frequencies of B97D are persistently too low, with a relatively large deviation from the experiment of 69 cm^{-1} in the case of B.

However, in the C=O stretching range the predictions for the spectral shifts upon dimerization are consistently similar for D_{het} and D_{hom} at each level of theory. Thus it is unlikely that the two dimer peaks D_C correspond to the two isomers. In the antisymmetric stretching region (B), the homochiral dimer would be expected to give rise to a secondary band in a region where we do not observe absorptions, but it may be too weak. In the symmetric stretching band region (A) (where no scaling to experiment is carried out due to the close vicinity of the B band), the homochiral dimer should give rise to a strong, slightly blue-shifted band, whereas the heterochiral dimer is expected to overlap more closely with the monomer. In summary, the spectra are consistent with the heterochiral dimer within the expected accuracy of the predictions, whereas the homochiral dimer is more at variance with the observations. The energetic prediction is to be weighted even more heavily in this case and suggests that the expansion only contains heterochiral C_i-symmetric dimers. Concerning the relative quality of the quantum chemical predictions, the experimental dimer positions fall about midway between the MP2 and B3LYP predictions, whereas B97D overestimates the dimerization effects in all regions.

There is one major discrepancy to be discussed. The predictions locate the IR-active C=O stretching transition of the dimer more or less in between the two observed D_C bands. As elaborated, there is no dimer structure available in the accessible energy window which would offer a conformer interpretation. This points to a Fermi resonance which is not captured in the harmonic approximation. Such Fermi resonances are quite abundant in the carbonyl stretching region (see below and ref. 12 and 17) and it is actually exceptional that it is absent in the particular case of ethylene carbonate monomer. There is one likely candidate for a perturbing combination tone visible in the spectrum of Fig. 2. Band B is significantly blue-shifted upon dimerization (D_B). If it is combined with the symmetric ring deformation vibration near 700 cm^{-1} (B3LYP/6-311++G(d,p)), the sum comes very close to the center of the two observed D_C bands (1855 cm^{-1}). Anharmonic calculations support a strong coupling between these three modes, whereas the corresponding monomer transitions are predicted nearly 50 cm^{-1} apart. For less likely Fermi resonance partners, see Table S2 in the ESI.† In the condensed phase, other resonances were also discussed.[17]

We will not discuss possible trimer assignments in detail, but just note that the sequence of average C=O red shifts for dimers (about 15 cm^{-1}), trimers (about 40 cm^{-1}) and the bulk

liquid (65 cm^{-1})[17] is monotonous. The sequence of blue shifts for the antisymmetric stretch saturates more quickly (29, 39, 37 cm^{-1}). As in the case of γ-butyrolactone,[12] such a behavior indicates a competing red-shifting coordination of the ring O-atoms in larger aggregates. This is also the case for the symmetric stretch red shift, where an almost negligible cluster effect (2 cm^{-1}) does not capture the liquid state trend (15 cm^{-1}). The latter finding is a strong indication for the absence of large clusters in our expansions. They should exhibit red shifts of at least 10 cm^{-1}. Furthermore, we note that the spread of the trimer C═O bands is consistent with the predicted strong excitonic coupling in these clusters. In the dimers, the splitting between the observed IR band and the Raman-active symmetric band is predicted around 20–25 cm^{-1}. Whether or not the Raman band will also be affected by an analogous Fermi resonance with the symmetric O–C–O stretching band remains to be seen.

In summary, the IR spectrum of EC shows that there is most likely a single heterochiral inversion-symmetric dimer in a pronounced case of complementary chirality synchronization between the transiently chiral C_2 monomers. The experimental spectrum is largely matched or bracketed by harmonic B3LYP, B97D and MP2 shift predictions at the 6-311++G(d,p) level, except for a pronounced Fermi resonance band with a coupling matrix element of 4 cm^{-1}. Verification of the structure, which has the two rings at a center of mass distance of about 321 pm, by microwave spectroscopy will be difficult, because the strong dipole moments cancel.[4]

It is worthwhile to analyze the cohesion energy (Table 1), which is predicted at 52.0 kJ mol^{-1} (MP2), 42.5 kJ mol^{-1} (B97D) or 26.5 kJ mol^{-1} (B3LYP). In the MP2 case, the purely electrostatic contribution amounts to 2/3 of the dissociation energy of the dimer, based on a distributed multipole analysis on the atoms of the distorted monomers (GDMA version 2.2.03[18] up to rank 5 with default settings, Orient version 4.6.09[19]). Both quantities obviously involve repulsive and attractive components. While it is clear that most of the cohesion is electrostatic, one may speculate about the role of two relatively short C–H···O contacts (2.53 Å) to the carbonyl oxygen atoms, but they are difficult to separate from electrostatic and dispersion contributions. However, they contribute 5% to the purely electrostatic attractive forces.

3.2 Propylene carbonate (PC)

After having characterized the monomer and dimer of EC, we can proceed to the more complex and more delicate case of PC. In addition to the transient chirality induced by ring twisting, the methylation of one of the ring carbon atoms introduces a more stable stereogenic center (see Fig. 1). The resulting transient diastereoisomerism is reflected by an axial or equatorial position of this methyl group. The chirodiastaltic energy is predicted at 1.1 (1.8) kJ mol^{-1} at the MP2 (B3LYP) level. The interconversion barrier is predicted at 4.5 kJ mol^{-1} (MP2 including zero point energy), still low enough for a likely stabilization of the most stable pair of enantiomers in the jet.

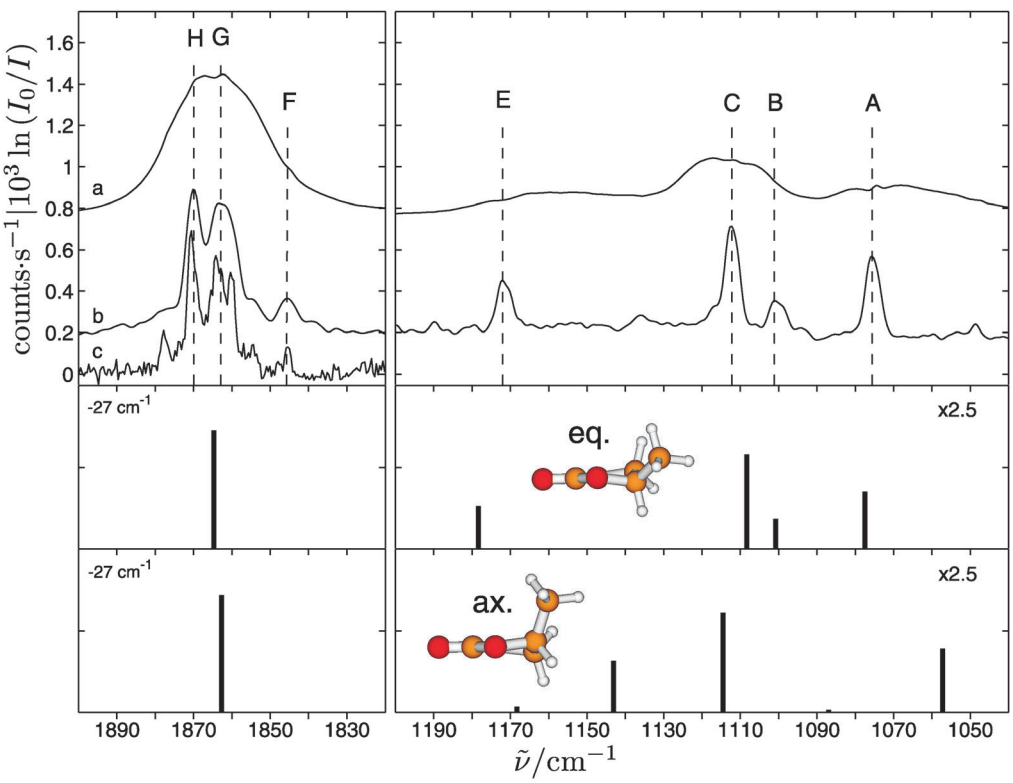

Fig. 4 Comparison of B3LYP/6-311++G(d,p) monomer wavenumber predictions for the equatorial and axial conformation of PC with the gas phase- (×0.033) (a) and high dilution jet spectrum (b). The calculated wavenumbers of the carbonyl stretching band are shifted by the same amount as in EC (Fig. 2). Also shown is a high dilution jet Raman spectrum (c) in the C═O range using the setup described in ref. 20. It reveals at least six components and the similarity in relative intensity to the IR counterparts suggests a Fermi resonance origin for most of them.

Indeed, the monomer-dominated jet spectrum (Fig. 4b) is consistent with rather complete conversion to the equatorial isomer (>80%), whereas the room temperature gas phase spectrum might be interpreted in terms of a somewhat larger axial constituent. However, the evidence is circumstantial because of the thermal broadening, which is efficiently removed in the jet spectrum. In addition to the symmetric CH_2–O stretching mode (A) and the asymmetric O–C–O stretch (C), there is now some intensity from CH_2–O wagging (B) and C–H bending modes (E), which helps to discriminate the two diastereoisomers. Furthermore, there is now a complex Fermi resonance pattern for the C═O stretching mode, which is only revealed at low temperature. It involves at least two perturbers F and H, which must be different from the EC dimer case, but shall not be analyzed in detail. A control experiment using Raman jet spectroscopy (see ref. 20 for a description, here we use moderate heating of the sample to 303 K and heating of the nozzle to 323 K) reveals at least six bands (see Fig. 4) which share the oscillator strength of the C═O stretching vibration. The higher resolution derives from the dominance of Q-branch intensity in the Raman transitions, but all peaks are also evidenced in the IR spectrum, partly as shoulders. The Fermi resonance interpretation is strongly supported by a similar intensity pattern in the Raman and IR spectra, which is consistent with a single bright (C═O) state. The center of gravity appears to be almost undistorted from the broad central band (G) in the FTIR jet spectrum, because F and H perturb from the right and left side, respectively. For comparison with theory, the calculated carbonyl stretching frequencies in Fig. 4 were shifted by the same value as for EC, which leads to good agreement with the experiment. Thus, the harmonic B3LYP frequencies for the carbonyl stretch show consistent deviations from the experiment for EC and PC.

All these spectral complications together with the racemic nature of the employed PC sample lead to a rather complex and delicate situation in the dimers, which has previously been overlooked.[5] Indeed, there is a multitude of cluster transitions which appear when one moves from the monomer-dominated expansion to the heated expansion (Fig. 5 for the C═O range, for the C–O range see Fig. S1 in the ESI†). Therefore, we have also studied a heated expansion for an enantiopure sample of PC. For the dimers, but not for larger clusters, a heterochiral spectrum (Fig. 5c) can be simulated by subtracting the enantiopure from twice the racemic spectrum, if dimer formation in the jet is irreversible and thus statistical with respect to stable stereogenic centers, as we usually observe it.[21]

There is a major difference for the strongest C═O stretching bands which are dimer-dominated. The synthetic heterochiral expansion contains two of these, whereas the enantiopure expansion only contains one, placed in between the other two and strongly overlapping with the least red-shifted one in the racemic expansion. Under the tentative assumption that the Fermi resonances are detuned in the dimer apart from minor components such as the one marked G + D, this indicates a single homochiral dimer, in analogy to the single heterochiral dimer of EC. In the spirit of Occam's razor, we will first try to assign the enantiopure spectra using only this singular dimer.

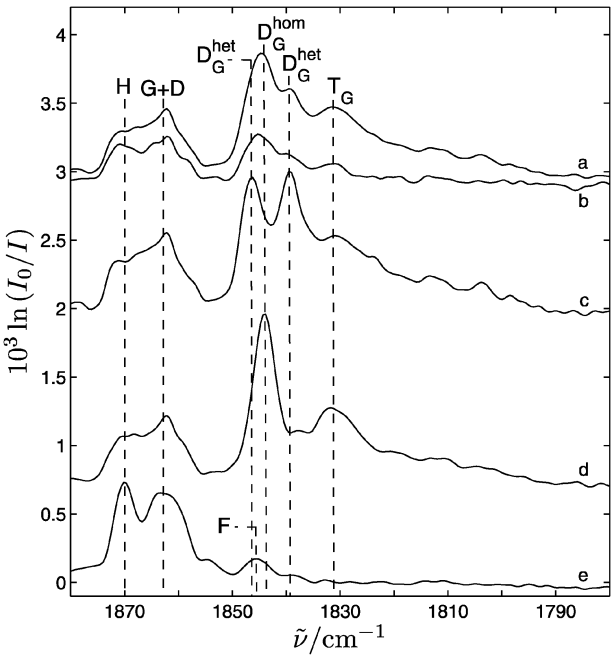

Fig. 5 Heated jet spectra of PC in the carbonyl range: Racemic PC at (a) 80 °C and (b) 50 °C; (c) synthetic heterochiral spectrum (2a–d); (d) enantiopure PC at 80 °C. (e) Monomer-dominated jet spectrum, 600 mm nozzle, ~1 bar stagnation pressure.

Numerous dimer geometries were found for PC, due to the above described complexity. In the most stable homochiral dimer found (D^{ae}_{hom}) only one molecule is in the favored equatorial conformation, while the other is forced into the axial conformation (Fig. 6). The next lowest homochiral dimer structure (D^{ae}_{hom2}) is relatively close in energy (Table 1), the difference being about 1.1 kJ mol^{-1} (MP2), 0.7 kJ mol^{-1} (B97D), or 0.2 kJ mol^{-1} (B3LYP). The spectral predictions for these two dimer geometries are nearly identical for the C═O range and very similar for the C–O range, which prevents an experimental differentiation between them. However, D^{ae}_{hom} already explains most of the peaks in the spectra, so further homochiral dimers are not required for consistency with the spectroscopic data.

The two heterochiral dimer structures displayed in Fig. 6 exhibit molecules with identical conformation within one cluster. The most stable heterochiral dimer D^{ee}_{het} features both molecules in the equatorial orientation and is energetically slightly favored over the lowest homochiral dimer (Table 1). The second best heterochiral structure D^{aa}_{het} is somewhat higher in energy (1.4 kJ mol^{-1} (MP2), 1.6 kJ mol^{-1} (B97D), 2.2 kJ mol^{-1} (B3LYP)) and contains both molecules in their axial conformation. These conformational differences lead to significant discrimination in the vibrational predictions, which enables comparison of both structures to the spectroscopic data. Another heterochiral dimer, which was previously described[13] with the monomers in different conformations (D^{ae}_{het}, not shown), features quite a narrow energy gap of 2.6 kJ mol^{-1} to the minimum structure at the B3LYP level, but is considerably less favored in the MP2 calculation with a relative energy of 7.7 kJ mol^{-1}. It could not be reproduced when using the B97D functional.

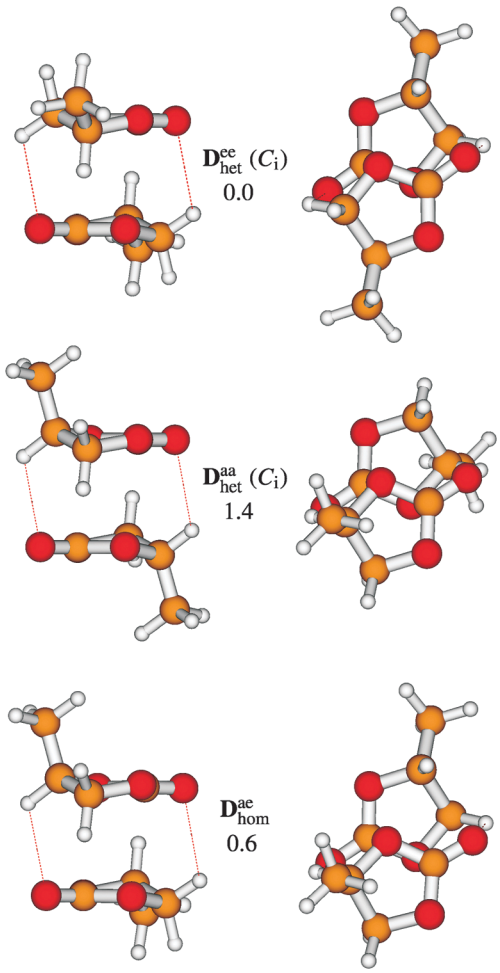

Fig. 6 Dimers of PC with relative MP2/6-311++G(d,p) energies ΔE_0 in kJ mol^{-1}, including zero-point correction.

Overall D^{ee}_{het}, D^{aa}_{het} and D^{ae}_{hom} are the only dimer structures of PC found within an energy window of 1.5 kJ mol^{-1} to the global minimum on the MP2 level. They resemble the EC dimer geometry, with antiparallel molecular dipole moments. In the cases of D^{ee}_{het} and D^{aa}_{het} the molecular dipole moments cancel each other out due to the inversion symmetry of the dimers, while for D^{ae}_{hom} a dipole moment of 0.89 D was found on the MP2 level. In the dimer geometries an exo orientation is favored over an endo position for the methyl group. Equatorial conformers form a C–H···O contact with the CH_2 group, while axial conformers dock *via* their CH group.

Fig. 7 shows experimental and theoretical results for the carbonyl stretching vibration of PC. The calculated wavenumbers have been shifted, so that the monomer bands coincide with G. Absolute shifts for each level of calculation are nearly identical for EC and PC, supporting the Fermi resonance interpretation.

D^{ae}_{hom} shows fair agreement with the measured dimer shifts on the B3LYP level. MP2 under- and B97D overestimates the dimer shift, like in the case of EC. The two dimer peaks in the heterochiral spectrum may be explained by the different dimers D^{ee}_{het} and D^{aa}_{het}, although B97D does not predict different shifts for the IR-active carbonyl stretch of the two structures

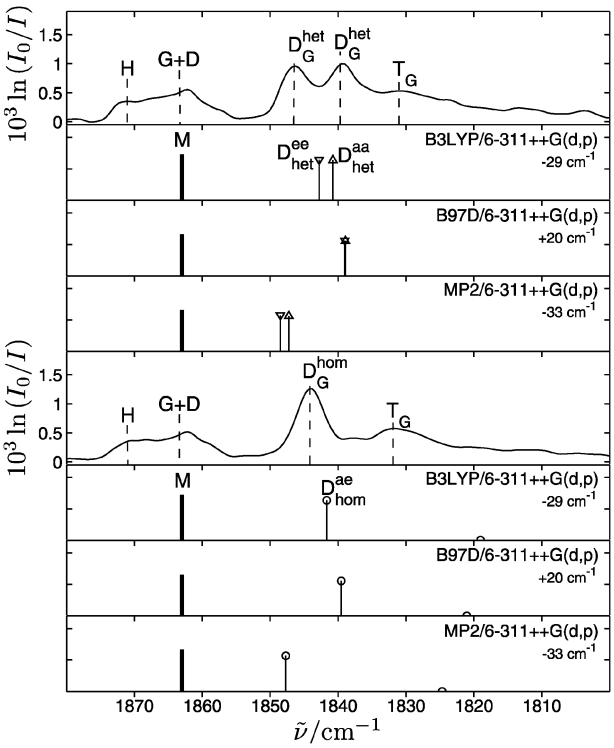

Fig. 7 Comparison between hetero- (upper half) and homochiral (lower half) dimer peaks of PC and corresponding calculations. Calculated wavenumbers were shifted by the displayed values, so that monomer bands coincide.

and the splitting between the two vibrations is still underestimated in the MP2 and B3LYP calculations. However, since the assignment of peaks in the C–O range (see Fig. S2 in the ESI†) points towards at least two heterochiral dimer species measured, it is more likely that the two dimer peaks of the carbonyl stretching vibration originate from different dimer structures present, rather than chirality specific anharmonic coupling through Fermi resonance. We emphasize that beyond the robust chirality recognition case, the spectral assignments in terms of one or two homo- and heterochiral PC dimers remains tentative in as much as they reach the limits of quantum chemical accuracy and band resolution. However, they provide a plausible and consistent assignment of an extended part of the infrared spectrum.

4 Conclusions

The dimers of EC and PC show analogous sandwich-like structures, in which the molecular dipole moments attract each other in antiparallel orientation. Similar results were also found for the related γ-butyrolactone.[12] C–H···O contacts only contribute weakly to the dissociation energy. A dimerization-induced Fermi resonance was found for EC. It gives rise to two C=O stretching bands despite a single centrosymmetric structure created by chirality synchronization. Owing to its permanent chirality and conformational flexibility three dimer structures of PC were assigned to the jet-cooled spectra. They involve monomers which differ either in their ring conformation, or in their absolute configuration,

but not in both at the same time. The energetic effects for these dimers are below the thermal energy at room temperature, but they are likely to be amplified in a closely packed fluid. Any molecular dynamics simulation of liquid EC and PC should be able to describe these subtle chirality recognition effects, if we are to trust it in the microscopic description of such battery solvents. Our results also indicate that chiral ionic solutes could be useful in fine tuning the electrochemical properties of PC. This may be valuable in elucidating ionic transport and transfer mechanisms or in organic catalysis. Finally, the high EC melting enthalpy of 0.15 kJ g^{-1} [22] is seen to have contributions from the ordered stacking of transiently chiral units, which is lost in the liquid state. Electrostatics prevents a high vapor pressure, thus making it suitable to store environmental heat and to capture CO_2 at the same time.

Acknowledgements

The present work was supported by the DFG research training group 782 (www.pcgg.de) and the Fonds der Chemischen Industrie. We thank Merwe Albrecht for valuable help and discussions and Nils Lüttschwager for providing a Raman jet spectrum of the PC monomer C=O stretching range (Fig. 4).

References

1 M. North, R. Pasquale and C. Young, *Green Chem.*, 2010, **12**, 1514–1539.
2 A.-A. G. Shaikh and S. Sivaram, *Chem. Rev.*, 1996, **96**, 951–976.
3 B. Schäffner, F. Schäffner, S. P. Perevkin and A. Börner, *Chem. Rev.*, 2010, **110**, 4554–4581.
4 J. L. Alonso, R. Cervellati, A. D. Esposti, D. G. Lister and P. Palmieri, *J. Chem. Soc., Faraday Trans. 2*, 1986, **82**, 337–356.
5 L. Borges Silva and L. C. Gomide Freitas, *THEOCHEM*, 2007, **806**, 23–34.
6 S. Grimme, *J. Comput. Chem.*, 2006, **27**, 1787–1799.
7 T. N. Wassermann, J. Thelemann, P. Zielke and M. A. Suhm, *J. Chem. Phys.*, 2009, **131**, 161108.
8 R. M. Balabin, *J. Phys. Chem. Lett.*, 2010, **1**, 20–23.
9 J. K. Choi and M. J. Joncich, *J. Chem. Eng. Data*, 1971, **16**, 87–90.
10 A. Borba, M. Albrecht, A. Gómez-Zavaglia, M. A. Suhm and R. Fausto, *J. Phys. Chem. A*, 2010, **114**, 151–161.
11 M. J. Frisch, G. W. Trucks, H. B. Schlegel, G. E. Scuseria, M. A. Robb, J. R. Cheeseman, G. Scalmani, V. Barone, B. Mennucci, G. A. Petersson, H. Nakatsuji, M. Caricato, X. Li, H. P. Hratchian, A. F. Izmaylov, J. Bloino, G. Zheng, J. L. Sonnenberg, M. Hada, M. Ehara, K. Toyota, R. Fukuda, J. Hasegawa, M. Ishida, T. Nakajima, Y. Honda, O. Kitao, H. Nakai, T. Vreven, J. A. Montgomery, Jr., J. E. Peralta, F. Ogliaro, M. Bearpark, J. J. Heyd, E. Brothers, K. N. Kudin, V. N. Staroverov, R. Kobayashi, J. Normand, K. Raghavachari, A. Rendell, J. C. Burant, S. S. Iyengar, J. Tomasi, M. Cossi, N. Rega, J. M. Millam, M. Klene, J. E. Knox, J. B. Cross, V. Bakken, C. Adamo, J. Jaramillo, R. Gomperts, R. E. Stratmann, O. Yazyev, A. J. Austin, R. Cammi, C. Pomelli, J. Ochterski, R. L. Martin, K. Morokuma, V. G. Zakrzewski, G. A. Voth, P. Salvador, J. J. Dannenberg, S. Dapprich, A. D. Daniels, O. Farkas, J. B. Foresman, J. V. Ortiz, J. Cioslowski and D. J. Fox, *Gaussian 09, Revision A.02*, Gaussian, Inc., Wallingford, CT, 2009.
12 S. Hesse and M. A. Suhm, *Phys. Chem. Chem. Phys.*, 2009, **11**, 11157–11170.
13 Y. Wang and P. B. Balbuena, *J. Phys. Chem. A*, 2001, **105**, 9972–9982.
14 P. D. Vaz and P. J. A. Ribeiro-Claro, *Struct. Chem.*, 2005, **16**, 287–293.
15 A. Zehnacker and M. A. Suhm, *Angew. Chem., Int. Ed.*, 2008, **47**, 6970–6992.
16 C. J. Brown, *Acta Crystallogr.*, 1954, **7**, 92–96.
17 B. Fortunato, P. Mirone and G. Fini, *Spectrochim. Acta, Part A*, 1971, **27**, 1917–1927.
18 A. J. Stone, *J. Chem. Theory Comput.*, 2005, **1**, 1128–1132.
19 A. J. Stone, A. Dullweber, O. Engkvist, E. Fraschini, M. P. Hodges, A. W. Meredith, D. R. Nutt, P. L. A. Popelier and D. J. Wales, *Orient: a program for studying interactions between molecules, version 4.6.09*, University of Cambridge, 2008, enquiries to A. J. Stone, ajs1@cam.ac.uk.
20 N. O. B. Lüttschwager, T. N. Wassermann, S. Coussan and M. A. Suhm, *Phys. Chem. Chem. Phys.*, 2010, **12**, 8201–8207.
21 N. Borho and M. A. Suhm, *Org. Biomol. Chem.*, 2003, **1**, 4351–4358.
22 M. S. Ding, K. Xu and T. R. Jow, *J. Therm. Anal. Calorim.*, 2000, **62**, 177–186.

